Demonstration and System Analysis of High Temperature Steam Electrolysis for Large-Scale Hydrogen Production Using SOFCs

8th European SOFC Forum

Michael G. McKellar
James E. O'Brien
Carl M. Stoots
J. Stephen Herring

July 2008

Idaho National Laboratory

Demonstration and System Analysis of High Temperature Steam Electrolysis for Large-Scale Hydrogen Production Using SOFCs

Michael G. McKellar, James E. OBrien, Carl M. Stoots, J. Stephen Herring
Idaho National Laboratory
P.O. Box 1625
Idaho Falls, Idaho 83415- 3710 / USA
Tel: 208-526-1346
Michael.McKellar@inl.gov

Abstract

High-temperature electrolysis (HTE) of steam holds the promise of efficient large-scale hydrogen production that does not require consumption of fossil fuels and, if based on nuclear energy or renewables, does not produce greenhouse gases. This technology is based on the use of solid-oxide electrolysis cells derived from solid-oxide fuel cells. A 15 kW integrated laboratory scale (ILS), HTE facility has been developed for research and technology demonstration. Initial operation of this facility resulted in over 400 hours of operation with an average hydrogen production rate of approximately 0.9 Nm^3/hr. The ILS facility is designed to address large-scale issues such as thermal management (feed-stock heating, high-temperature gas handling, heat recuperation), multiple-stack hot-zone design and manifolding, multiple-stack electrical configurations, hydrogen recycle, and other "integral" issues. A parallel system-analysis activity is also under way in which a reference process model of a commercial-scale high-temperature electrolysis plant for hydrogen production has been developed. The reference plant design is driven by a 600 megawatt thermal high-temperature helium-cooled reactor coupled to a direct Brayton power cycle. The overall system thermal-to-hydrogen production efficiency (based on the low heating value of the produced hydrogen) is 47.1% at a hydrogen production rate of 2.36 kg/s with the high-temperature helium-cooled reactor concept. This paper documents the initial operation of the ILS, with experimental details about heat-up, initial stack performance, as well as long-term operation and stack degradation. The paper will also present the optimized design for the reference nuclear-driven HTE hydrogen production plant which may be compared with other hydrogen production methods and power cycles to evaluate relative performance characteristics and plant economics.

Introduction

Dwindling US oil reserves, decreasing reliability of foreign crude oil, and increasing concerns about greenhouse gas emissions have created a strong interest in developing alternative energy sources, particularly for the transportation and shipping industries [1]. One such technology is hydrogen generation via high temperature steam electrolysis. Hydrogen can be produced by water splitting via HTE without greenhouse gas emissions if the process is powered by nuclear energy. Due to the high efficiency of the HTE process, the overall hydrogen production efficiency is close to the thermal efficiency of the electric power source. The high reactor outlet temperatures expected from the next generation of

nuclear plants [2] can provide the high-temperature process heat and the power cycle thermal efficiency that will promote the HTE process hydrogen production efficiencies greater than 50%.

Research on HTE has been under way at the Idaho National Laboratory for several years [3 - 14]. The research effort includes experiments, modeling, and simulation. Experimental activities have included testing of single button cells (~2 watt) [3], short stacks (~ 500 watt) [4], and the integrated laboratory scale facility (~15 kilowatts) [5]. Electrolysis testing has included steam, carbon dioxide, and combined steam/carbon dioxide co-electrolysis [6 - 10] for the direct production of syngas. Modeling and simulation work has included detailed computational fluid dynamics [11] simulations and process flow modeling. Three-dimensional computational heat transfer and fluid models of the solid oxide electrolysis cells (SOEC) and stacks have been developed and parametric studies performed to analyze steam electrolysis and combined steam/CO2 co-electrolysis. A mole fraction and temperature-averaged high temperature steam and/or carbon dioxide electrolysis process flow model was also developed for use in a commercial process modeling code [12, 13]. This electrolysis model combined with process models of next generation and current nuclear plants are used to determine overall hydrogen production efficiencies, nuclear process heat integration, and heat recuperation opportunities.

This paper will provide results of the experimental work on the integrated laboratory scale system and on the process modeling work using next generation nuclear plants. The areas of computational fluid dynamics and co-electrolysis at the INL are presented in other papers within this forum.

Overview of Integrated Lab Scale Facility

The INL integrated lab scale HTE facility includes three electrolysis modules (see Fig. 1), with 4 planar SOEC stacks per module, and 60 planar solid oxide cells per stack. Each cell has an active area of 64 cm^2. The modules are designed to operate in cross flow. Fig. 1(a) shows the hydrogen/steam mixture inlet, the steam/hydrogen outlet, and the sweep air inlet manifolds. The air/oxygen flow exits through the front and back open faces. The internal components of the stack are shown in Fig. 1(b). The interconnect plate is made from ferritic stainless steel and includes an impermeable separator plate with edge rails and two corrugated flow fields: one for the sweep gas and the other for the feed

Figure 1. (a) ILS 4-stack module; (b) solid-oxide stack components

Table 1. ILS Single Module Design Parameters

Independent Design and Operational Parameters		Anticipated Performance Values	
Active Cell Area	64 cm^2	Per-cell Operating Voltage	1.283 V
Cells per Stack	60	Current Density	0.25 A/cm^2
Number of Stacks	4	Stack Power	1232 W
Stack Operating Temperature	830°C	Total Power (Electric)	4.85 kW
Steam Utilization	50%	Inlet Hydrogen Flow Rate	5.8 NLPM
Stack Operating Voltage	77 V	Inlet Steam Flow Rate	53 NLPM
Per-cell ASR	1.5 Ω·cm^2	Inlet Liquid Water Flow Rate	0.7 g/s
Inlet Steam Mole Fraction	0.9	Air Flow Rate	22.6 NLPM
Inlet Hydrogen Mole Fraction	0.1	Hydrogen Production Rate	1578 NL/hr
		Heating Value of Hydrogen	4.7 kW

gas. The steam/hydrogen and air sweep flow fields are fabricated from nickel foil and ferritic stainless steel respectively. To improve performance, the sweep-side separator plates and flow fields are surface-treated to form a rare-earth stable conductive oxide scale. A perovskite rare-earth coating is also applied to the separator plate oxide scale by either screen printing or plasma spraying. On the steam / hydrogen side of the separator plate, a thin (~10 µm) nickel metal coating is applied. The electrolyte is scandia-stabilized zirconia, ~140 µm thick. The sweep-side electrode (anode in the electrolysis mode) is a strontium-doped manganite. The electrode is graded, with an inner layer of manganite/zirconia (~13 µm) immediately adjacent to the electrolyte, a middle layer of manganite (~18 µm), and an outer bond layer of cobaltite. The steam / hydrogen electrode (cathode in the electrolysis mode) is also graded, with a nickel cermet layer (~13 µm) immediately adjacent to the electrolyte and a pure nickel outer layer (~10 µm).

Each pair of stacks is called a half module. To preclude the loss of an entire stack if a single cell fails, the four stacks are electrically interconnected at every fifth cell. When the two half-modules are placed back-to-back, a common air inlet plenum for all four stacks is formed. Spring-loaded compression bars are placed over the stacks to maintain a compressive load on the stacks during operation. Power leads to each stack, intermediate voltage taps and interior thermocouples are attached to the stack via the accessible air outlet faces. Sealing of the air inlet plenum completed the installation. A summary of ILS module specifications is provided in Table 1.

The three ILS modules are placed in a single hot zone enclosure and each module is fed by one of three independent systems that supplies feedstock, sweep gas streams, and electrical power. Fig. 2 is the piping and instrumentation schematic for a single ILS module. The steam/hydrogen feedstock is shown in magenta, the orange lines represent the product streams, the inlet sweep gas stream is green, and the outlet sweep gas is shown in blue. Liquid water flows at a controlled rate into the system through a Coriolis mass flow controller. The water is then vaporized and slightly superheated in an inline electrically-powered steam generator. The steam generator outlet temperature is feedback-controlled. The steam is mixed with hydrogen (about 10%) to maintain reducing conditions at the hydrogen/steam electrode. During startup, the hydrogen is supplied from a compressed gas bottle. During steady operation, the hydrogen can be recycled from the product stream. The hydrogen flow rate is fixed by a mass-flow controller via the data acquisition and control system. Downstream of the mixing point, temperature, pressure and dew point of the inlet process stream are measured. Precise measurement of the
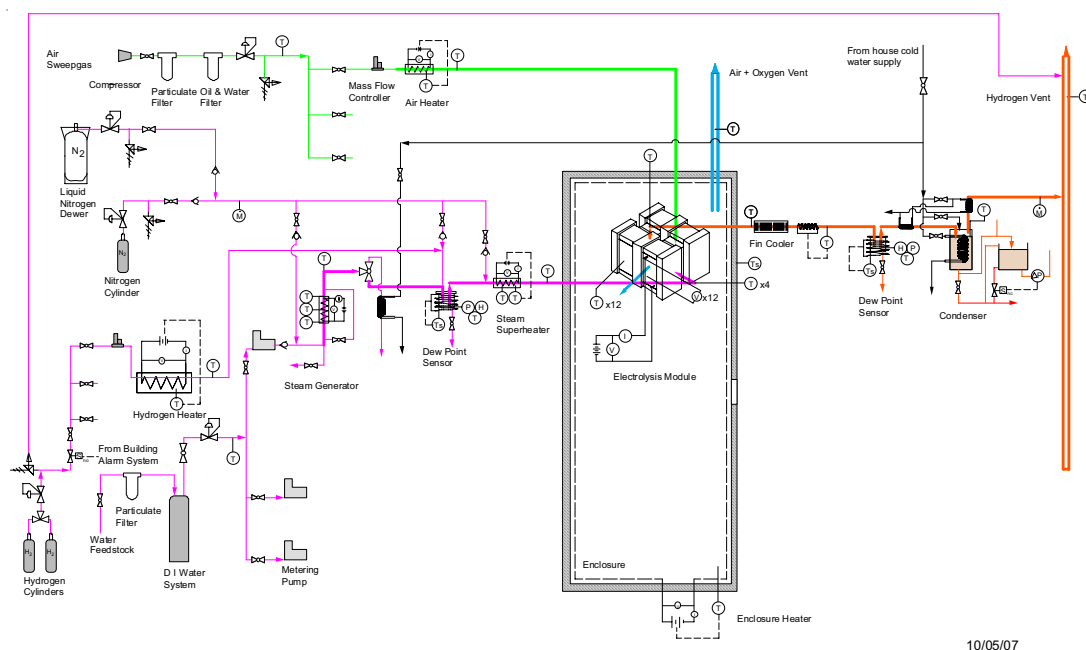
3

Figure 2. ILS single-module piping and instrumentation schematic.

dewpoint and the pressure provide an independent determination of the inlet gas composition. A high-temperature inline electrically-powered superheater increases the temperature of the feedstock stream to 800 – 830°C.

The primary material for the low-temperature tubing and components is 316 stainless steel. For the high temperatures, Inconel 600 tubing is used. The hot zone enclosure maintains the desired operating temperatures using radiant heaters installed in the sides and top of the removable lid (Fig. 3). The modules rest on top of an insulated stainless steel plate. The process streams, power leads, and instrumentation access the modules through holes in the bottom plate. The mixture leaving the electrolyzer is enriched with hydrogen, typically at least 50% mole fraction with the remainder as steam. The product stream is cooled in a natural convection air-cooled heat exchanger to a point where no

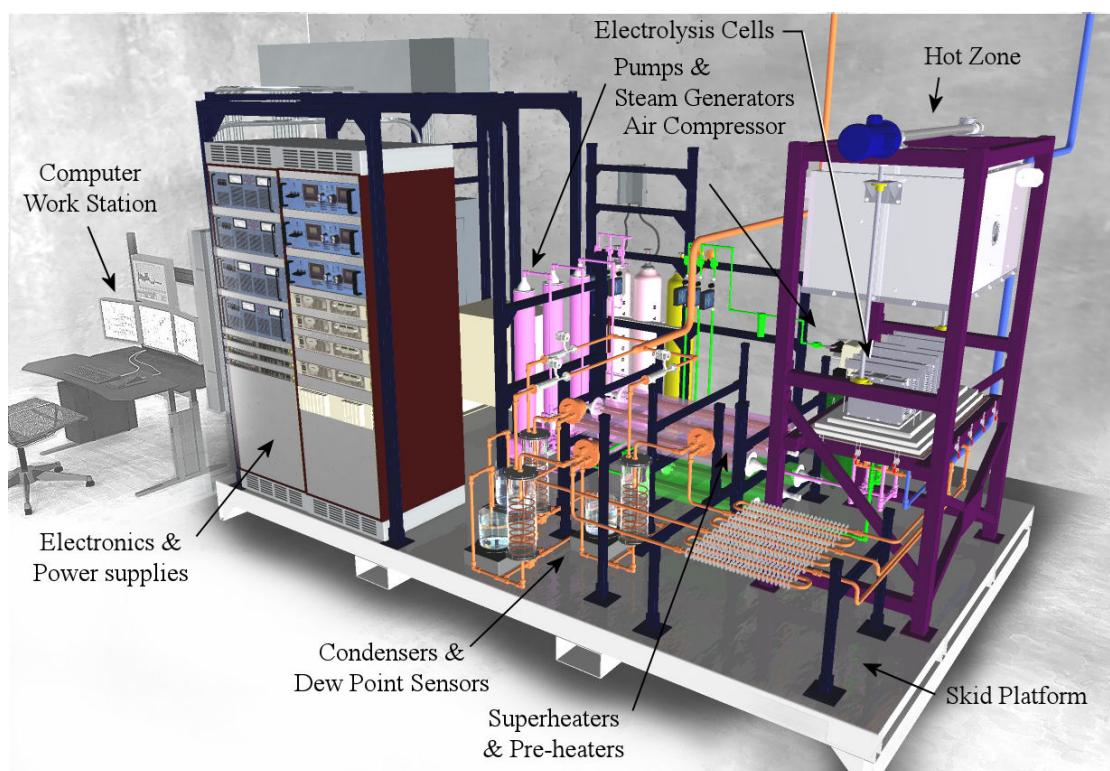Figure 3. Hot zone enclosure with one module installed.

4

Figure 4. INL ILS facility, with major components labelled.

condensation occurs. The dewpoint of the product gas mixture is then measured to determine steam consumption and hydrogen production rates. These rates are compared to the electrochemical hydrogen production rate determined from the stack electrical current. A condenser is used to remove the residual steam from the product stream. The flow rate of the hydrogen exit stream, (~2.7% residual water vapor) is measured with a mass-flow meter and then the stream is vented from the building. Air is used as an oxygen sweep gas. The air is filtered, compressed and heated before flowing into the hot zone. The exiting oxygen-enriched air stream from the hot zone is vented outside the building.   Nitrogen is injected into the steam superheater during startup to prevent liquid from entering the electrolysis module. Nitrogen may also be used to reduce hydrogen diffusion rates during steady state conditions by increasing the average molecular weight of the gas. All of the system components and hardware are mounted on a 3 m × 5 m skid. A labelled rendering of the overall ILS system is presented in Fig. 4 .

Table 3. Test Operating Conditions

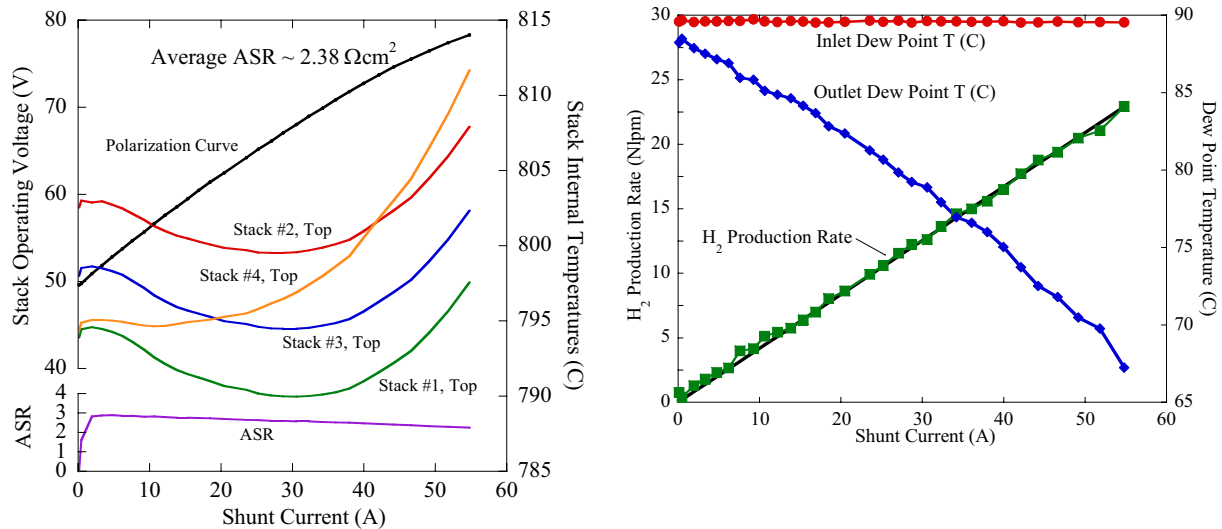|	
Hot Zone Temperature	820 C
Inlet Water Mass Flow Rate	34 ml/min
Inlet Hydrogen Flow Rate	5.4 Nl/min
Inlet Nitrogen Flow Rate	5.4 Nl/min
Inlet Air Flow Rate	25 Nl/min
Measured inlet dew point	91.3 C

Figure 5. (a) ILS module voltage sweep / polarization curve; (b) ILS module voltage sweep hydrogen production rates and dew points

ILS Single-Module Test Results

Two initial tests were performed with the single-module integrated lab scale system: a voltage sweep test and a long-duration test [5]. Operating conditions for both tests are listed in Table 3. The voltage sweep test was performed after the ILS had been running for 27 hours. During the sweep, the power supply voltage was varied between 50 to 79 V (0.83 V/cell to 1.32 V/cell) which corresponds to operating between open-cell voltage to slightly above thermal neutral. The voltage / current or polarization curve is shown in Fig. 5(a). The average per-cell area specific resistance, ASR, for this test was 2.38 $\Omega \cdot cm^2$,
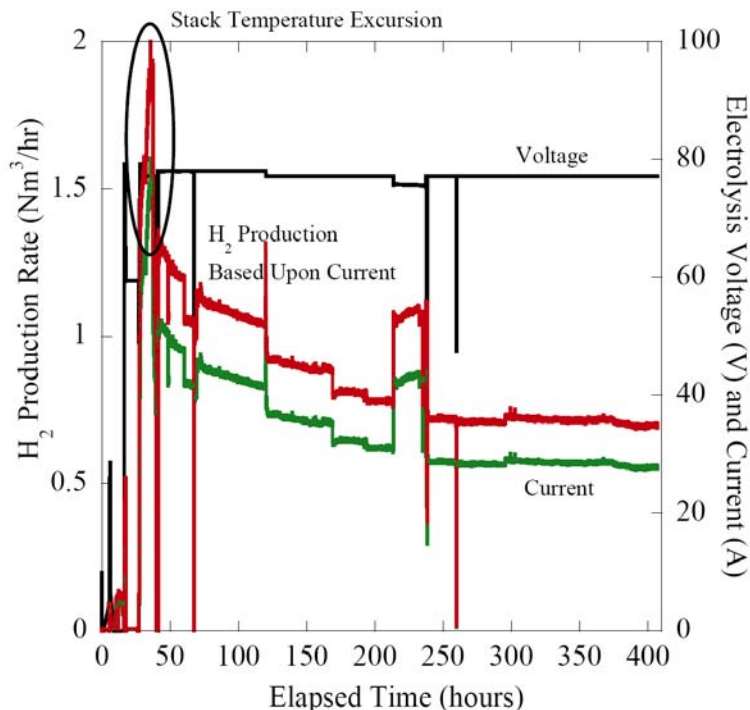

Figure 6. Complete electrical history of ILS single-module long-durationtest.

6

which was much higher than expected. Stack internal temperatures initially decrease as the voltage increases due to the dominance of the endothermic heat of reaction. As the voltage increases beyond the thermal neutral point, outlet temperatures exceed the inlet temperatures. Fig. 5(b) shows the inlet and outlet dewpoint temperatures and hydrogen production rate for the ILS single-module sweep.   The inlet dewpoint temperature remained constant for the duration of the test. The outlet dewpoint decreased as the current increased due to the increase in hydrogen production. The black line in Fig. 5(b) is the calculated hydrogen production rate based on the electrolysis current which corresponds well with the dewpoint-based hydrogen production rate shown in green. At the highest current levels, the hydrogen production rate exceeded 1.5 Nm^3/hr.

Fig. 6 shows the results from the long-endurance test, performed under a constant-voltage operating condition at 1.3 V/cell. The test continued for 420 hours and was concluded after about 250 hours, after stack performance degradation had stopped. During the test, the hydrogen production rate dropped from an initial value of 1.5 Nm^3/hr to 0.7 Nm^3/hr. A primary focus of the HTE research at INL is to minimize this performance degradation.

Reference Commercial-Scale Nuclear-Driven HTE Hydrogen Production Plant

A process model of a commercial-scale high temperature electrolysis production plant has been developed at the INL.   The HTE hydrogen production plant uses a very high temperature gas reactor (VHTR) to supply both heat and power to the electrolysis process. The primary advantage of high temperature electrolysis over conventional electrolysis, which is a well established technology, is that considerably higher overall efficiencies can be achieved.   The improved performance of HTE versus conventional low-temperature (alkaline or PEM) electrolysis is due to both the improved power-cycle efficiencies and electrolyzer efficiencies associated with high-temperature operation. Higher reactor outlet temperatures yield higher power-cycle efficiencies in accordance with the Carnot principle. The electrolyzer itself benefits from high-temperature operation for reasons related to both thermodynamics and kinetics.   From thermodynamics, the electrical energy requirement for water or steam electrolysis decreases with increasing temperature, while the thermal energy requirement increases. Consequently, at higher temperatures, a larger fraction of the total electrolysis energy input can be supplied in the form of heat, increasing the overall process efficiency.   In terms of kinetics, activation and ohmic electrochemical overpotentials also decrease dramatically with temperature.

UniSim process-analysis software was used to evaluate the performance of the commercial-scale hydrogen production plant coupled to a high temperature helium-cooled reactor. UniSim inherently ensures mass and energy balances across all components and it includes thermodynamic data for all chemical species. The work described in this paper establishes an optimized reference design based on analyses of process flow diagrams that include realistic representations of the reactor power source coupled to the Brayton power cycle integrated with the high-temperature electrolysis process loops.   As with previous HTE system analyses performed at the INL, a custom electrolyzer model was incorporated into the overall process flow sheet [12]. This electrolyzer model allows for the determination of the average Nernst potential, cell operating voltage, gas outlet temperatures, and electrolyzer efficiency for any specified inlet steam, hydrogen, and sweep-gas flow rates, current density, cell active area, and external heat loss or gain. The electrolyzer model has been validated by comparison with results obtained from a fully 3-D computational fluid dynamics model and by comparison with experimental results.

7

The process flow diagram for the very high-temperature helium-cooled reactor coupled to the direct helium Brayton power cycle and the HTE plant with air sweep is presented in Fig. 7. The power cycle loop showing the reactor coupled to the direct helium recuperated Brayton cycle is presented in the lower left of Fig. 7. This UniSim power-cycle model was initially described in [14]. The primary helium coolant exits the reactor at 900°C. This helium flow is split at T1, with more than 85% of the flow directed toward the power cycle and the remainder directed to the intermediate heat exchanger to provide process heat to the HTE loop. Within the power-cycle loop, helium flows through the power turbine where the gas is expanded to produce electric power. The helium, at a reduced pressure and temperature, then passes through a recuperator and precooler where it is further cooled before entering the low-pressure compressor. To improve compression efficiencies, the helium is again cooled in an intercooler heat exchanger before entering the high-pressure compressor. The helium exits the high-pressure compressor at a pressure that is slightly higher than the reactor operating pressure of 7 MPa. The coolant then circulates back through the recuperator where the recovered heat raises its temperature to the reactor inlet temperature of 540°C, completing the cycle.
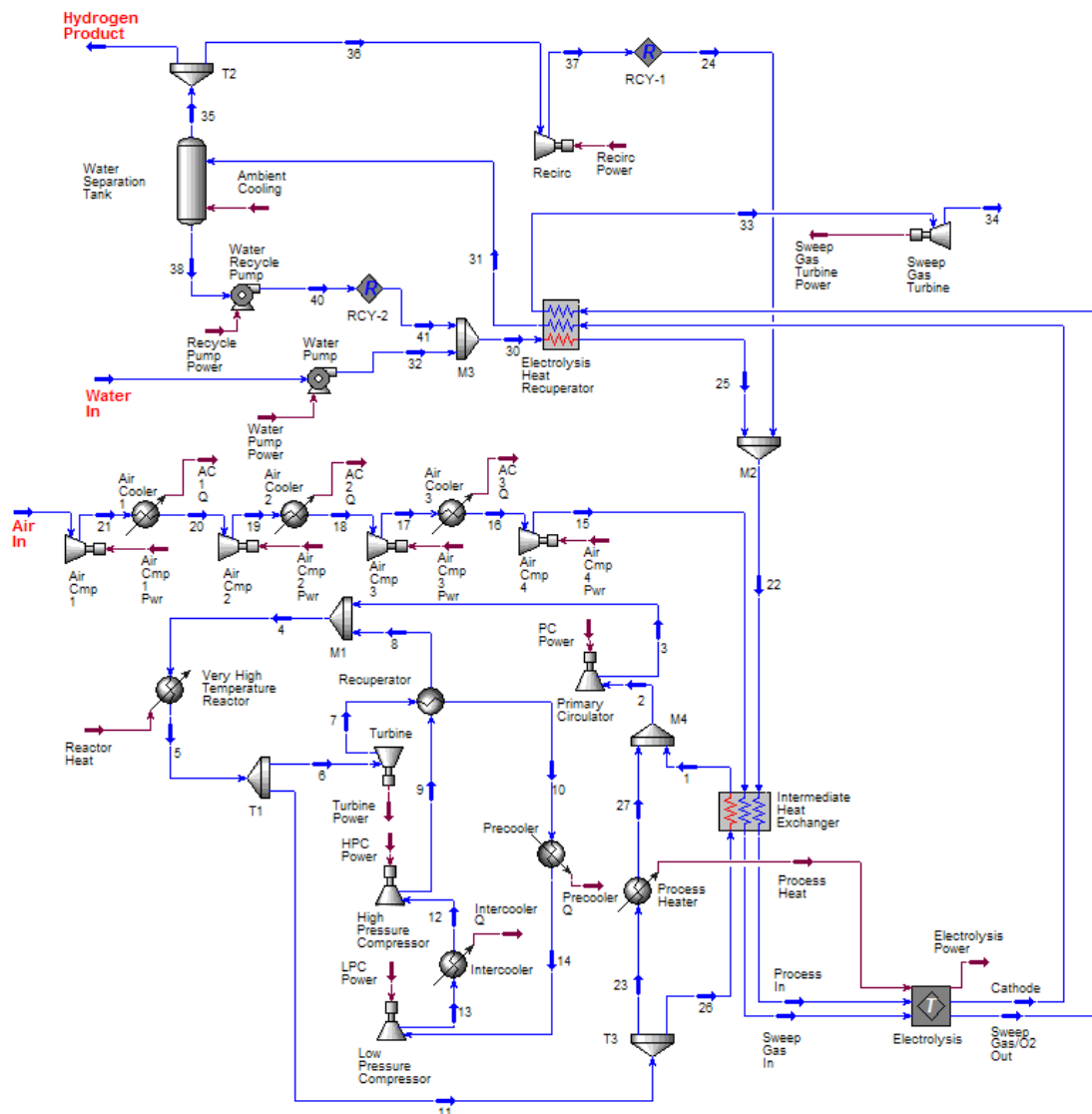

Figure 7.   Process flow diagram for helium-cooled reactor/direct Brayton/HTE system with air sweep.

Process heat for the HTE hydrogen production plant is provided by splitting the reactor coolant outlet flow into two streams, and allowing a fraction (typically less than 15%) of the flow to pass through an intermediate heat exchanger where heat is extracted for use in the hydrogen production process. The cooler helium leaving the intermediate heat exchanger (stream 3 in Fig. 7) is then returned through a circulator to the reactor inlet pressure and mixed with the primary coolant returning to the reactor. The reactor thermal power assumed for the high-temperature helium-cooled reactor was 600 MW_{th}. The UniSim-calculated power cycle thermal efficiency for the power cycle represented in Fig. 7 is 53.2 %.

For the HTE process, the liquid water feedstock enters at the left in Fig. 7. The water is then compressed to the HTE process pressure of 5.0 MPa in the liquid phase using a pump. Downstream of the pump, condensate from the water knockout tank is recycled back into the inlet stream at M3. The water stream is then vaporized and pre-heated in the electrolysis recuperator, which recovers heat from the post-electrolyzer process and sweep-gas outlet streams. Downstream of the recuperator, at M2, the steam is mixed with recycled hydrogen product gas. A fraction of the product gas is recycled in this way in order to assure that reducing conditions are maintained on the steam/hydrogen electrode. Downstream of the mixer, the process gas mixture enters the intermediate heat exchanger (IHX), where final heating to the electrolysis operating temperature occurs, using high-temperature process heat from the nuclear reactor. The process stream then enters the electrolyzer, where oxygen is electrolytically split from the steam, producing hydrogen and oxygen. An additional process heater is used to directly add heat during the electrolysis process to maintain isothermal electrolyzer operating conditions. The custom electrolyzer module developed at INL for direct incorporation into the UniSim system analysis code has been described in detail previously [12].

Downstream of the electrolyzer, the hydrogen – rich product stream flows through the electrolysis recuperator where the product stream is cooled and the inlet process stream is preheated. The product stream is cooled further at the water knockout tank, where the majority of any residual steam is condensed and separated, and yielding dry hydrogen product. The cooled product stream is split at T2 and a fraction of the product gas is recycled into the inlet process stream, as discussed previously. A recirculating blower is required to repressurize the recycle stream to the upstream pressure at M2.

The process flow diagram shows air in use as a sweep gas, to remove the excess oxygen that is evolved on the anode side of the electrolyzer. In the air sweep system, inlet air is compressed to the system operating pressure of 5.0 MPa in a four-stage compressor with intercooling. The final compression stage is not followed by a cooler, so the air enters the IHX at about 171°C. The sweep gas is heated to the electrolyzer operating temperature of 800°C via the IHX which supplies high-temperature nuclear process heat directly to the system. The sweep gas then enters the electrolyzer, where it is combined with product oxygen. Finally, it passes through the electrolysis recuperator to help preheat the incoming process gas. Some of the sweep gas compression work is recovered using a sweep-gas turbine located at the sweep-gas exit. Because the electrolyzer uses DC current, the conversion from AC to DC must be accounted. For this reference case we have assumed a conservative AC-to-DC conversion efficiency of 96%.

The per-cell active area for electrolysis was assumed to be 225 cm^2. This cell size is well within the limits of current technology for planar cells. The total number of cells used in the reference design was determined by specifying a current density of 0.25 A/cm^2, an area-

9

specific resistance, *ASR*, value of 0.4 $\Omega \cdot cm^2$ and assuming isothermal conditions for the electrolysis process. The number of cells was adjusted until the full power cycle output at this operating point is dedicated to electrolysis. This procedure resulted in 4.01×10^6 cells required. The *ASR* value of 0.4 $\Omega \cdot cm^2$ used in the electrolyzer model is based on the current industry-best achievable *ASR* for solid oxide fuel cells. For this model, the inlet composition of the feed stream was specified as 90% steam and 10% water. The electrolysis process converted 88.9% of the steam to hydrogen and oxygen, resulting in an outlet composition of 90% hydrogen and 10% steam.

To allow for comparisons between the performances of the HTE process to alternate hydrogen production techniques, we have adopted a general efficiency definition that can be applied to any thermal water-splitting process, including HTE, low-temperature electrolysis (LTE), and thermochemical processes. Since the primary energy input to the thermochemical processes is in the form of heat, the appropriate general efficiency definition to be applied to all of the techniques is the overall thermal-to-hydrogen efficiency, η_H. This efficiency is defined as the heating value of the produced hydrogen divided by the total thermal input required to produce it. In this report, the lower heating value, LHV, of the produced hydrogen has been used:

$$\eta_H = \frac{LHV}{\sum_i Q_i} \tag{1}$$

The denominator in this efficiency definition quantifies all of the net thermal energy that is consumed in the process. For a thermochemical process, this summation includes the direct nuclear process heat as well as the thermal equivalent of any electrically driven components such as pumps, compressors, etc. The thermal equivalent of any electrical power consumed in the process is the power divided by the thermal efficiency of the power cycle. For the reference helium-cooled direct Brayton cycle, the power-cycle thermal efficiency is 53.23%. For the electrolysis process, the summation in the denominator of Eqn. (1) includes the thermal equivalent of the primary electrical energy input to the electrolyzer and the secondary contributions from smaller components such as pumps and compressors. In additional, any direct thermal inputs are also included. Direct thermal inputs include any net (not recuperated) heat required to heat the process streams up to the electrolyzer operating temperature and any direct heating of the electrolyzer itself required for isothermal operation. Finally, if the reactor outlet temperature is insufficient to raise the feed temperature to the desired electrolyzer operating temperature (in this case 800°C), then the thermal equivalent of any auxiliary heaters must be included. If these heaters use electrical resistance heat, the heat input is penalized by the power cycle thermal efficiency. If the heaters are combustion-based, only the direct heat amount is included. An auxiliary heater was not required for the reference case described in this report, since the reactor outlet temperature is 900°C and the electrolyser operates at 800°C. For the reference design case, the predicted overall thermal-to-hydrogen efficiency is 47.12%. If the AC to DC conversion efficiency is assumed to be 100%, the efficiency increases to 48.76%.

Using the UniSim model, a parametric study was performed in which the current density was adjusted to see the effect on the system. Figs. 8(a) and 8(b) show the results of this parametric study. In each case, the total power of the reactor was dedicated to hydrogen production via HTE. To achieve this, the number of cells in the electrolyzer had to be adjusted. As shown in Fig. 8(a), as the current density is increased, the overall hydrogen production efficiency and the corresponding hydrogen production rate decreases. Furthermore, the overall hydrogen production efficiency decreases about 1.5% if an AC-to-DC conversion factor of 96% is assumed. Although higher efficiencies may be achieved at
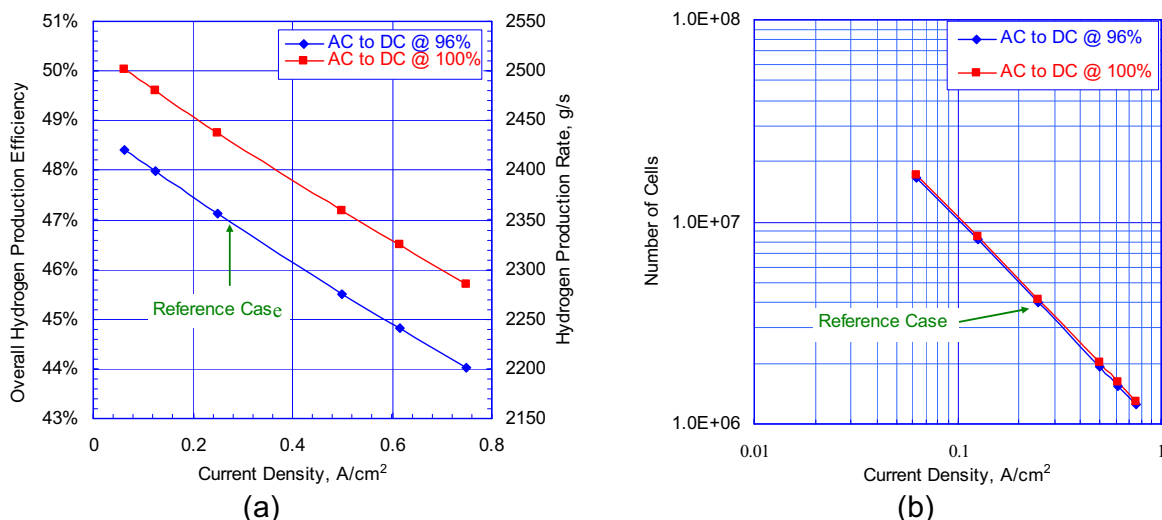
10

(a)　　　　　　　　　　　　　　　　　(b)

Figure 8. (a) Overall hydrogen production efficiency and rate as a function of current density; (b) number of electrolyzer cells required for full reactor power utilization.

lower current densities, the required number of cells also increases (for full reactor power utilization) which has a direct impact on the capital cost of the electroylzer, see Fig. 8(b).

Additional process models have been developed in which the HTE process was combined with other nuclear reactor types so that the effect of the reactor outlet temperature could be quantified. In this analyses, two additional reactor power cycles were developed, a sodium-cooled reactor combined with a steam Rankine power cycle, and a supercritical carbon dioxide-cooled reactor combined with a recuperated Brayton power cycle. These same reactor power cycles were also used to drive a low temperature electroyzler (LTE) process. Results plotted in Fig. 9 indicate higher overall hydrogen production efficiencies for higher reactor outlet temperatures. In addition, the HTE process is more efficient than LTE for each reactor type/outlet temperature considered, by about 10 percentage points. Each reactor type was considered over an appropriate temperature range for its design. The LTE process is always less efficient than the high temperature electrolysis process, because the LTE process does not take advantage of direct heat input to improve the steam splitting process.   It is interesting to note that the nuclear reactor with the supercritical carbon dioxide Brayton power cycle has better performance than the helium cooled reactor at temperatures ranging from 700 to 800 C. The power cycle efficiency of the helium-cooled reactor drops rapidly as the temperature decreases.

Conclusions

This paper provides an update on recent experimental and modeling research activities under way at the Idaho National Laboratory on high-temperature electrolysis.   This process is being considered for efficient large-scale carbon-free nuclear-powered hydrogen production. Results of experimental studies to date have indicated that HTE represents a promising near-term technology for this application.   However, cell performance and degradation must be improved before commercial-scale deployment can occur. System modeling results summarized in this paper indicate that an overall thermal-to-hydrogen efficiencies greater than 50% can be achieved for HTE coupled to advanced high-temperature reactors.
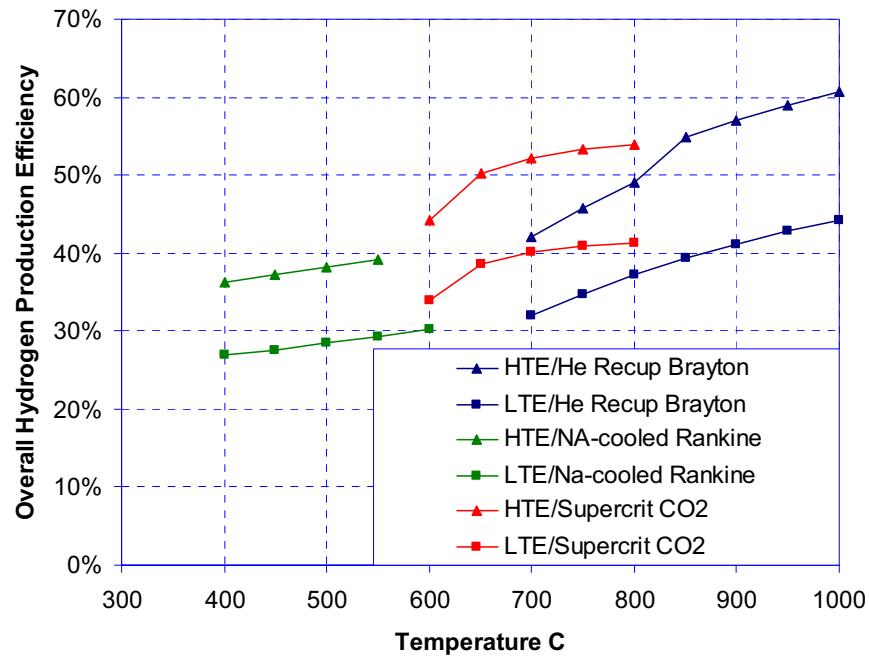
Figure 9. Overall hydrogen production efficiency as a function of reactor outlet temperature.

Acknowledgements

Copyright Statement

References

(1) Forsberg, C. W., "The Hydrogen Economy is Coming. The Question is Where?" *Chemical Engineering Progress*, December, 2005, pp. 20-22.

(2) Southworth, F. H., Macdonald, P. E., Harrell, D. J., Park, C. V., Shaber, E. L., Holbrook, M. R., and Petti, D. A., "The Next Generation Nuclear Plant (NGNP) Project," Proceedings, Global 2003, pp. 276-287, 2003.

(3) O'Brien, J. E., Stoots, C. M., Herring, J. S., Lessing, P. A., Hartvigsen, J. J., and Elangovan, S., "Performance Measurements of Solid-Oxide Electrolysis Cells for Hydrogen Production from Nuclear Energy," *Journal of Fuel Cell Science and Technology*, Vol. 2, pp. 156-163, August 2005.

(4) O'Brien, J. E., Stoots, C. M., Herring, J. S., and Hartvigsen, J. J.,"Hydrogen Production Performance of a 10-Cell Planar Solid-Oxide Electrolysis Stack," *Journal of Fuel Cell Science and Technology*, 3, pp. 213-219, (2006).

(5) Condie, K.G., Stoots, C.M., O'Brien, J.E., and Herring, J.S., "Characterization of the Transient Response of the ILS with One Module Installed to Heatup Changes in Power Level and Cooldown," INL Technical Report INL/EXT-07-13626, December, 2007.

(6) O'Brien, J.E., Stoots, C., Herring, J.S., and Hartvigsen, J., "High-Temperature Co-electrolysis of Carbon Dioxide and Steam for the Production of Syngas: Equilibrium Model and Single-Cell Tests," paper no. 173084, ANS Embedded Topical: International Topical Meeting on the Safety and Technology of Nuclear Hydrogen Production, Control, and Management, June 24 - 28, 2007, Boston, Massachusetts, USA.

(7) Stoots, C.M., O'Brien, J.E., and Hartvigsen, J., "Test Results of High Temperature Steam/CO2 Coelectrolysis in a 10-Cell Stack," paper no. 173131, ANS Embedded Topical: International Topical Meeting on the Safety and Technology of Nuclear Hydrogen Production, Control, and Management, June 24 - 28, 2007, Boston, Massachusetts, USA.

(8) Hawkes, G.L., O'Brien, J.E., Stoots, C.M., Herring, S.J., and Hartvigsen, J., "3D CFD Model of High Temperature H2O/CO2 Co-Electrolysis," paper no., 173216, ANS Embedded Topical: International Topical Meeting on the Safety and Technology of Nuclear Hydrogen Production, Control, and Management, June 24 - 28, 2007, Boston, Massachusetts, USA.

(9) O'Brien, J.E., Stoots, C.M., Hawkes, G.L., Herring, J.S., and Hartvigsen, J., "High-Temperature Coelectrolysis of Steam and Carbon Dioxide for Direct Production of Syngas: Equilibrium Model and Single-Cell Tests," Fifth International Conference on Fuel Cell Science, Engineering & Technology, June 18-20, 2007, New York, USA.

(10) Stoots, C. M., O'Brien, J. E., "Results of Recent High-Temperature Co-electrolysis Studies at the Idaho National Laboratory," paper # 412b, 2007 AIChE Annual Meeting, Salt Lake City, November 4 – 9, 2007.

(11) Hawkes, G. L., O'Brien, J. E., Stoots, C. M., Herring, J. S., "CFD Model of a Planar Solid Oxide Electrolysis Cell for Hydrogen Production from Nuclear Energy," *Nuclear Technology*, Vol. 158, pp. 132 - 144, May, 2007.

(12) O'Brien, J. E., Stoots, C. M., and Hawkes, G. L., "Comparison of a One-Dimensional Model of a High-Temperature Solid-Oxide Electrolysis Stack with CFD and Experimental Results," Proceedings, 2005 ASME International Mechanical Engineering Congress and Exposition, Nov. 5 – 11, Orlando.

(13) O'Brien, J. E., McKellar, M. G., Hawkes, G. L., and Stoots, C. M., "Development of a One-Dimensional Co-Electrolysis Model for Use in Large-Scale Process Modeling Analysis," Fifth International Conference on Fuel Cell Science, Engineering & Technology, June 18-20, 2007, New York, USA.

(14) Harvego, E. A., McKellar, M. G., O'Brien, J. E., and Herring, J. S., "Summary of Reactor-Coupled HTE Modeling Sensitivity Studies," DOE Milestone Report, INL internal report# INL/INT-06-11889, October 26, 2006.